Surface Science 158 (1985) 165–189
North-Holland, Amsterdam

PHOTOPHYSICS AND PHOTOCHEMISTRY NEAR SURFACES AND SMALL PARTICLES *

Joel I. GERSTEN

Department of Physics, City College of the City University of New York, New York, New York 10031, USA

and

Abraham NITZAN

Department of Chemistry, Tel Aviv University, Tel Aviv 69978, Israel

Received 3 September 1984

The optical response of molecucules adsorbed at or near interfaces are known to be strongly modified relative to those of the free molecules. Surface-enhanced Raman scattering is the most prominent example, however practically all molecular optical properties are affected. In this paper we review the electromagnetic theory of these phenomena with particular emphasis on resonance processes. We discuss lifetimes of excited molecular states, absorption, resonance Raman and fluorescence cross-sections, light scattering and emission yields, energy transfer between adsorbed molecules and photochemical processes. The electromagnetic theory of these phenomena incorporates the surface effect on the local electromagnetic field intensity with the surface-induced radiative and nonradiative decay rates to give working expressions for cross-sections, rates and yields of surface optical processes in terms of the incident beam direction, polarization and frequency, geometry and optical properties of the substrate and its environment and of the optical properties, location and orientation (relative to the substrate) of the adsorbed molecule. Available experimental results are in good qualitative or semiquantitative agreement with the theory. In addition we consider the role of cavity sites in surface-enhanced optical processes. We discuss two models for cavity sites, the conical wedge and enclosures between small particles. The latter are shown to be associated with particularly large enhancements both of the local field intensity and of the surface-induced radiative and nonradiative decay rates. Finally we dwell on the optical properties of small molecular particles which, near the molecular resonance, may give rise to strong local field enhancement provided that the molecules respond coherently to the incident radiation field. We show that the overall response depends on the rate of dephasing processes, which act to drive molecules out of phase with each other. The actual enhancements depend on this rate and on the particle size and shape.

1. Introduction

Surface-enhanced Raman scattering (SERS) [1] has been the most dramatic example of what we may call surface-enhanced spectroscopy. This includes a

* Supported in part by the United States–Israel Binational Science Foundation, Jerusalem, Israel, and by the Professional Staff Congress-Board of Higher Education faculty research award program of the City University of New York.

host of phenomena which are related to the strong modification of the optical properties of molecules adsorbed on dielectric (mostly metal) surfaces. Thus radiative and nonradiative relaxation rates of excited molecules states increase sharply near metal surfaces and depend strongly on the molecule–surface separation and on the molecular orientation [2,3]. Resonance Raman scattering [4–6] and fluorescence [5–10] are also enhanced although to a lesser extent (in fact the florescence signal of molecules with high fluorescence yields may be smaller near the surface [5]). The quantum yield for these processes (measuring the ratio between the scattering or fluorescence cross-sections and the absorption cross-sections) is strongly modified near the surface. Photochemical yields have been predicted to be enhanced under appropriate conditions near rough dielectric surfaces, and these predictions were recently verified experimentally [12–14]. Finally energy-transfer rates and yields are also expected to be strongly modified for donor and acceptor molecules adsorbed on metal or other dielectric surfaces [15].

The electromagnetic theory of surface-enhanced spectroscopy [11,16–31] provides an interpretation of the phenomena outlined above in terms of the surface-induced change in the local EM field near the surface and of the surface-induced radiative and nonradiative decay rates and level shifts of excited molecular states which combine additively with the decay rates and shifts associated with the bulk molecule. The change in the local field intensity is due to the image field [16,17], to excitation of electromagnetic resonances localized in particles and surface roughness features [18–23], to excitation of propagating surface plasmons in gratings [24–28] and in surfaces with small roughness [29,30] and to the lightning rod effects [19]. Excluding the image contribution which is known to be small [32,33] the other field enhancement models depend on some form of surface roughness, and predict enhancements in a distance range of about the order of the scale of the roughness.

Surface-induced radiative and nonradiative relaxation rates result from the electromagnetic interaction between the excited adsorbed molecule and surface plasmons and electron–hole pair excitation in the substrate. These depend strongly on the surface morphology [20,34], however, their dependence on the molecule–surface distance d is essentially the same as for flat surfaces: local dielectric theory [2] predicts a d^{-3} behavior at distances small relative to the radiation wavelength while nonlocal theory was recently used [3] to predict a d^{-4} dependence at distances small relative to the electronic mean free path in the substrate. The different distance dependence of the competing enhancement and damping mechanisms results in a more complicated distance behavior of all resonance optical processes [35] as detailed in sections 4 and 6 below.

Another complication arises, particularly for resonance optical processes, when the adsorbate coverage is high enough to affect the optical properties of the adsorbate molecule and of the dielectric substrate. This has a substantial effect on the coverage dependence of SERS [36] and dramatically changes the

optical response of systems with nearly lying substrate and adsorbate optical resonances (e.g., splitting of spectral lines and a complicated dependence on the substrate layer thickness) [7,9,37–39].

In this paper we describe several aspects of surface-enhanced spectroscopy, focusing on the electromagnetic theory and on resonance optical processes. It should be kept in mind that in addition to the (relatively long range) EM interactions chemisorption may have a strong influence on the optical properties of the adsorbate–substrate system due, e.g., to the appearance of new excited states. The appearance of such charge-transfer states for pyridine and pyrazine chemisorbed on Ag(111) [40] has been suggested as a factor in SERS of these sytems. Such chemical effects are system-specific and the magnitude of their effect on the optical properties of chemisorbed molecules is not known [44].

In what follows we first discuss the lifetimes of excited molecular states near rough surfaces and clusters of small particles and the local EM field intensity near such structures. We then discuss the implications of these phenomena for resonance optical processes involving molecules adsorbed on such surfaces. We discuss rates and yields of adsorption, resonance Raman, fluorescence, energy transfer and photochemistry. In this paper we also discuss the optical properties of small (50–1000 Å) molecular clusters and their possible use as substrates in surface-enhanced fluorescence.

2. Lifetimes

Consider a molecule represented by a point polarizable particle located at position $\boldsymbol{R}_M(=R_M, \theta_M, \phi_M)$ near a dielectric surface with the orientation of its transition dipole given by the angles θ_μ, ϕ_μ (the particular choice of coordinates depend on the geometry of the system). Close to resonance with a particular molecular transition the molecule may be represented by a classical point particle of polarizability α_M. α_M is related to the molecular radiative decy rate in vacuum, $\Gamma_R^{(f)}$ by

$$\alpha_M = \tfrac{3}{2}\left(c/\omega_M^{(f)}\right)^3 \Gamma_R^{(f)}/\omega_M^{(f)}, \tag{1}$$

where $\omega_M^{(f)}$ is the transition frequency of the free molecule and c is the speed of light. Near the surface the equation of motion of the molecular dipole, μ_M, may be taken to be of the Drude form

$$\ddot{\mu}_M + \left(\omega_M^0\right)^2 \mu_M + \gamma_M^0 \dot{\mu}_M = \left(\omega_M^0\right)^2 \alpha_M \, \boldsymbol{E}(\boldsymbol{R}_M, t) \cdot \mu_M/\mu_M, \tag{2}$$

where ω_M^0 and γ_M^0 are the molecular frequency and width in the bulk (the latter is generally a sum $\gamma_M^0 = \Gamma_R^0 + \Gamma_{NR}^0$ of radiative and nonradiative contributions) and where $\boldsymbol{E}(\boldsymbol{R}_M, t)$ is the local electric field at the molecule. The

Fourier component

$$\boldsymbol{E}(\boldsymbol{R}_{\mathrm{M}}, \omega) = \int \mathrm{d}t\, \boldsymbol{E}(\boldsymbol{R}_{\mathrm{M}}, t) \exp(\mathrm{i}\omega t)$$

is given by the general form

$$E(\boldsymbol{R}_{\mathrm{M}}, \omega) = \left[I + A(\boldsymbol{R}_{\mathrm{M}}, \omega)\right] \cdot \boldsymbol{E}_0(\boldsymbol{R}_{\mathrm{M}}, \omega) + G(\boldsymbol{R}_{\mathrm{M}}, \omega) \cdot \mu_{\mathrm{M}}(\omega), \tag{3}$$

where $\boldsymbol{E}_0$ is the incident field, I is the unit tensor, $A\boldsymbol{E}_0$ is the field at the molecule due to the polarization of the substrate by the incident field (see section 3) and where $G \cdot \boldsymbol{\mu}_{\mathrm{M}}$ is the field at the molecule caused by the polarization of the substrate by the molecular diople. Inserting (3) into the Fourier transform of (2) we obtain

$$\left(\omega_{\mathrm{M}}^2 - \omega^2 - \mathrm{i}\omega\gamma_{\mathrm{M}}\right) \mu_{\mathrm{M}}(\omega)$$

$$= \alpha_M \left(\omega_M^0\right)^2 (\mu_M/\mu) \cdot \left[I + A(\boldsymbol{R}_M, \omega)\right] \cdot \boldsymbol{E}_0(\boldsymbol{R}_M, \omega), \tag{4}$$

$$\omega_{\mathrm{M}}^2 = \left[\omega_{\mathrm{M}}^0 + \Delta\omega_{\mathrm{M}}^{(\mathrm{s})}(\omega)\right]^2, \quad \gamma_{\mathrm{M}} = \gamma_{\mathrm{M}}^0 + \gamma_{\mathrm{M}}^{(\mathrm{s})}(\omega), \tag{5}$$

where $\Delta\omega_{\mathrm{M}}^{(\mathrm{s})}$ and $\gamma_{\mathrm{M}}^{(\mathrm{s})}$ are the surface-induced level shift and width given by

$$\Delta\omega_{\mathrm{M}}^{(\mathrm{s})} = \omega_{\mathrm{M}}^{(0)} \left[1 - \alpha_{\mathrm{M}} \boldsymbol{n}_\mu \cdot \mathrm{Re}\; G(\boldsymbol{R}_{\mathrm{M}}, \omega) \cdot \boldsymbol{n}_\mu\right]^{1/2} - \omega_{\mathrm{M}}, \tag{6}$$

$$\gamma_{\mathrm{M}}^{(\mathrm{s})} = (\alpha_{\mathrm{M}}/\omega)\left(\omega_{\mathrm{M}}^0\right)^2 \boldsymbol{n}_\mu \cdot \mathrm{Im}\; G(\boldsymbol{R}_{\mathrm{M}}, \omega) \cdot \boldsymbol{n}_\mu, \tag{7}$$

where $\boldsymbol{n}_\mu = \boldsymbol{\mu}_{\mathrm{M}}/\mu_{\mathrm{M}}$ is a unit vector in the direction of the molecular transition moment [45]. Close to the molecular resonance we can replace ω by ω_{M} in eqs. (6) and (7).

The calculation of the surface-induced level shift and width is now reduced to the calculation of the tensor G which depends strongly on the molecular position and orientation with respect to the surface and on the surface geometry and dielectric properties. Ref. [2] reviews this calculation for a flat surface within local dielectric response theory while ref. [3] discusses nonlocal corrections to the nonradiative part, $\Gamma_{\mathrm{NR}}^{(\mathrm{s})}$, of $\gamma_{\mathrm{M}}^{(\mathrm{s})}$.

Results for simple nonplanar geometries have been also obtained [20,34] in the electrostatic approximation which is valid if all the characteristic distances in the system are much smaller than the radiation wavelength. In this approximation one first evaluates, from the Laplace equation, the field $\boldsymbol{E}(\boldsymbol{r}, \omega_{\mathrm{M}})$ induced in the substrate by the molecular dipole. The rate of energy loss in the substrate is

$$\left(\frac{\mathrm{d}W}{\mathrm{d}t}\right)_{\mathrm{NR}} = \tfrac{1}{2} \int_{\mathrm{sub}} \mathrm{d}\boldsymbol{r}\, \sigma(\boldsymbol{r}, \omega_{\mathrm{M}}) \left|\boldsymbol{E}(\boldsymbol{r}, \omega_{\mathrm{M}})\right|^2,$$

where $\sigma(\boldsymbol{r}, \omega) = (\omega/2\pi)\ \mathrm{Im}\ \epsilon(\boldsymbol{r}, \omega)$ is the substrate conductivity ($\epsilon(\boldsymbol{r}, \omega)$ being the substrate dielectric function at position $\boldsymbol{r}$) and where $\int_{\mathrm{sub}}$ denote an

integral over the substrate volume. The total radiative emission rate is

$$(\mathrm{d}W/\mathrm{d}t)_{\mathrm{R}} = (\mathrm{c}/3)(\omega_{\mathrm{M}}/c)^4 \left|\mu^0_{\mathrm{tot}}\right|^2,$$

where

$$\mu_{\mathrm{tot}} = \mu^0_{\mathrm{M}} + \frac{1}{4\pi}\int_{\mathrm{sub}} \mathrm{d}r\, \left[\epsilon(r, \omega_{\mathrm{M}}) - 1\right] E(r, \omega_{\mathrm{M}})$$

(the second term is the dipole induced in the substrate, μ^0 denotes the amplitude of $\mu(t) = \mu_0 \exp(-\mathrm{i}\omega_{\mathrm{M}} t)$). The total radiative and surface-induced nonradiative relaxation rates are then obtained by dividing respectively the

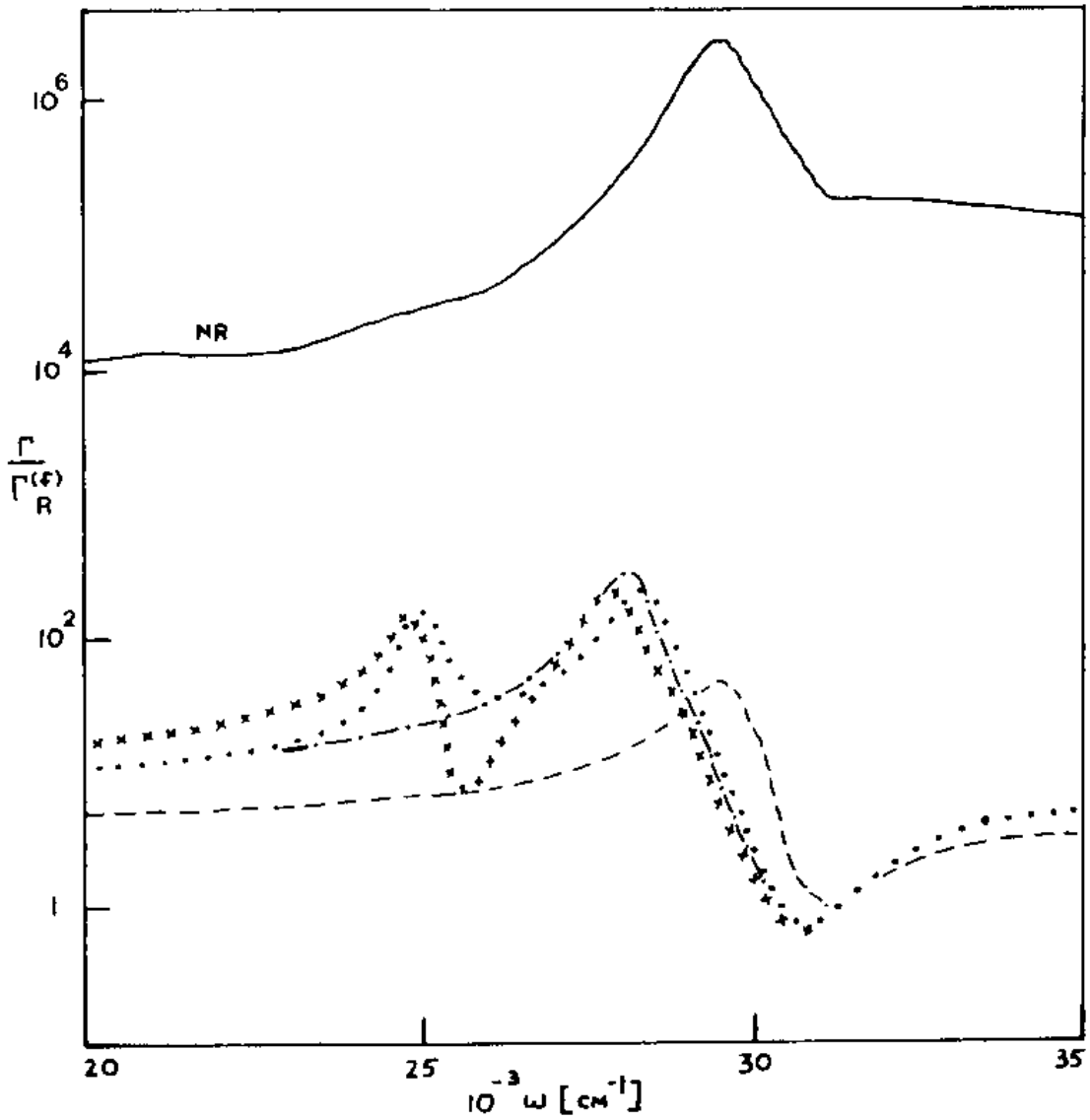

Fig. 1. Radiative and nonradiative relaxation rates of a molecule 5 Å from a silver surface with its transition dipole perpendicular to the surface. The surface is the plane surface of bulk silver or a spherical particle of radius 100 Å. The radiative rates are strongly configuration dependent: (— — —), molecule on a plane; (– · –), molecule on a single sphere; (· · · · · ·), molecule on a sphere with another identical sphere located nearby with the intersphere axis perpendicular to the molecule-sphere axis and the intersphere distance 210 Å; (× × ×), same, with the molecule located on the intersphere axis. The nonradiative rates (———) for all these configurations cannot be distinguished on this plot.

radiative, $(dW/dt)_R$, and nonradiative, $(dW/dt)_{NR}$, power losses by the total molecular energy $W_M = (\mu_M^0)^2/2\alpha_M$.

Using this method one can rederive the flat surface results obtained earlier [2] and extend them to several important nonplanar situations. The results for $\Gamma_R^{(s)}$ and $\Gamma_{NR}^{(s)}$ for a molecule located near a dielectric ellipsoid (or a sphere as an important limiting case) are given in ref. [20]. Another important model is that of a molecule adsorbed on a cluster of dielectric particles [34], which may be taken as several neighboring islands on a metal island film or as an aggregate of colloid particles.

Calculations based on these models show that the surface-induced radiative relaxation rate is strongly sensitive to the geometry of the substrate surface. The nonradiative relaxation rate also depends on this geometry but to a lesser extent. As long as the molecule–surface distance is much smaller then the length characterizing the nonplanarity of the surface (e.g., a molecule at a distance d from the surface of a sphere of radius a with $d \ll a$) the nonradiative lifetime is given to a good approximation by the planar surface result. Only when the molecule–surface distance is larger or when the molecule is enclosed between several surfaces (i.e. in a cavity site [46]) does the nonradiative lifetime become strongly dependent on the surface geometry.

As an example we show in fig. 1 the total radiative and the surface-induced nonradiative decay rates as functions of the molecular frequency ω for for different surface geometries. The nonradiative rates are almost identical in all cases while the total emission rates from the system vary considerably.

3. Local field enhancement

Much of the physics of enhanced photoprocesses on surfaces or on small particles is associated with the enhanced local fields present in the vicinity of such structures. Underlying this physics are various effect which often act in concert to determine the degree of enhancement. These are: (1) the high polarizability of small particles (or surface protrusions) when the frequency of the incident or emitted radiation (or other characteristic frequencies) coincides with electronic or ionic resonances of the structures; (2) the ability for sharp structures to concentrate electric field lines into a confined space (the lightning rod effect [19]); (3) the image charges induced when a molecule is in proximity to a conductor; and (4) the ability for particles of moderate size to efficiently radiate photons or, in the case where a substrate is present to radiate delocalized surface plasmons [50], and thereby open up additional damping channels. In some earlier work we studied the behavior of a molecule in the vicinity of a single spheroidally shaped particle and developed theories relating to SERS [19] and to fluorescence lifetimes and yields [20]. However, experimental conditions are often such as to make it necessary to consider clusters of

two or more particles in close proximity [51]. The qualitative insights obtained from the single-particle case may be used to develop a qualitative understanding of the more general case, and this will be our task here. On the other hand, to obtain a quantitative understanding one may utilize powerful Green function techniques [46,34,52].

Recent experiments on SERS [51] have indicated that strong local field enhancements are associated with cavity sites on rough surfaces. Furthermore, these enhancements may be stronger than those associated with the tips of isolated protrusions or single particles. One simple model for a cavity site consists of simply a conical pit indenting the surface. Since Laplace's equation is analytically solvable for this case one may estimate the degree of field enhancement if any, that occurs. We have done so [46] and find that there is not a strong enhancement. The pit acts basically to exclude rather than concentrate flux lines. Hence such a model is inadequate. Instead, we will model the cavity sites as the void spaces between clusters of spheres resting on a surface. In order to explain the origin of these strong fields let us begin by studying a configuration of two spheres. This problem has been studied quantitatively using the bispherical coordinate system [53], but here we shall simply sketch a qualitative treatment.

A conducting sphere placed in a uniform electric field exhibits some ability to concentrate the electric field, as is shown in fig. 2a. To a crude approximation one may regard two neighboring spheres as if they were encapsulated in a virtual prolate spheroid as shown in fig. 2b. For simplicity's sake it is convenient to take the direction of the incident field and the orientation of all molecular dipoles parallel to the symmetry axis. If the spheroid were indeed of uniform composition and characterized by a dielectric constant, ϵ, the field inside would be constant and the strongest field would be just outside the spheroid's tip. (Note that for $|\epsilon| \gg 1$ continuity of the normal component of electric displacement vector requires this.) Since, however, the composition of the virtual spheroid is not uniform the flux lines will be most concentrated in the region between the spheres, as is shown in fig. 2b. In this region we have a superposition of two concentrated fields, one from each sphere. At other points there is at most one concentrated field. Thus comparing points A, B and C one would expect point A, the cavity site, to possess the strongest local field and point C to have the weakest field. Extending this reasoning to a linear array of uniformly spaced spheres would suggest that the field would be strongest in the void at the center of the configuration. One may say that the outer spheres pre-focus the field lines and the inner spheres sharpen the focus further. In a similar fashion, a triangle composed of three spheres may be encapsulated by a virtual oblate spheroid and the field would be expected to be strong in the interior region, as is shown in fig. 2c. Thus quite generally, we may expect local fields in the void spaces of clusters of spheres to be quite strong.

The resonant character of a collection of spheres may be deduced from

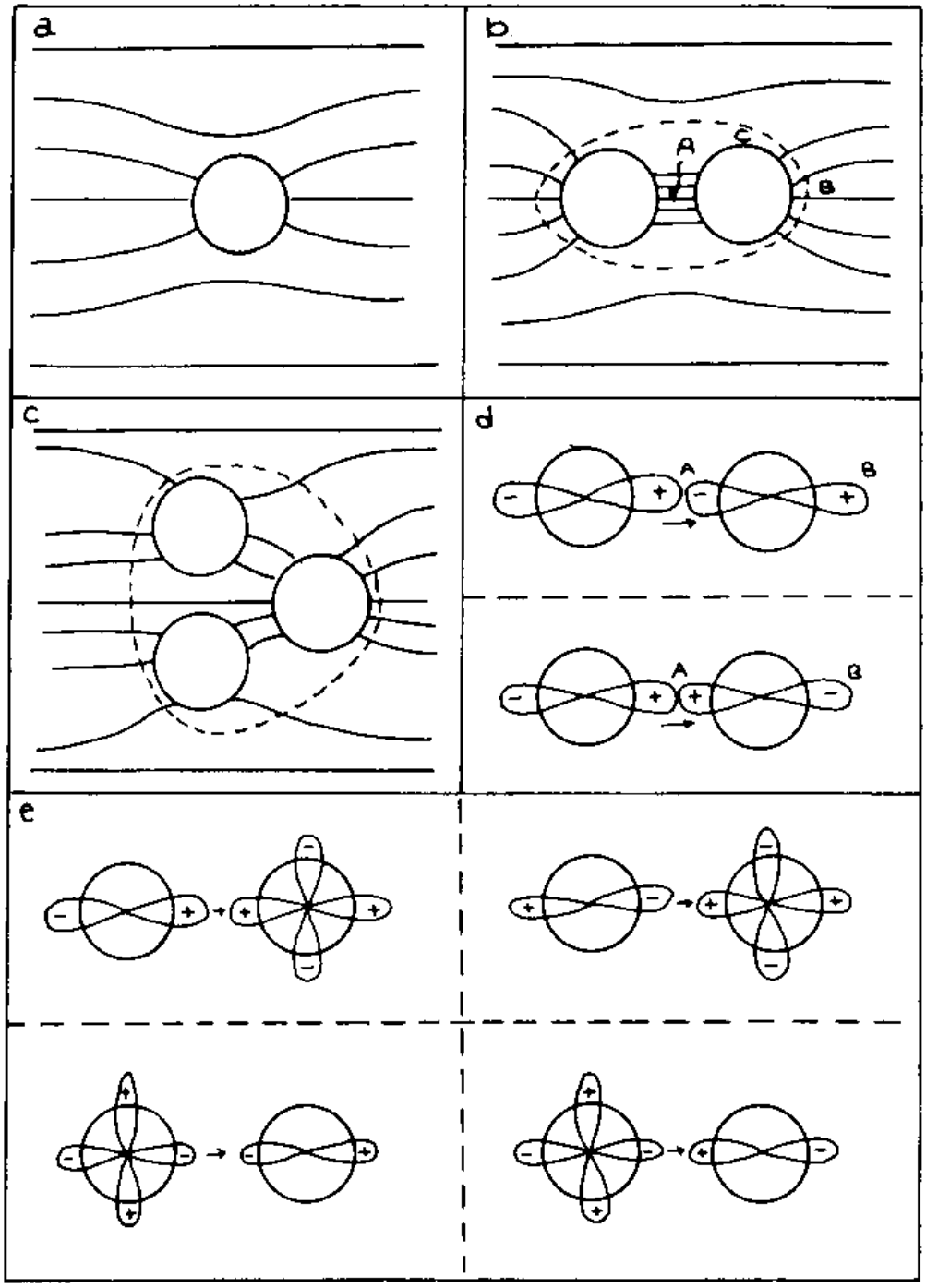

Fig. 2. (a) Electric field configuration near an isolated sphere. (b) Field near a two-sphere cluster. Dashed curve is the virtual prolate spheroid. (c) Field near a three-sphere cluster. Dashed curve is the equatorial plane of an oblate spheroid. (d) Electrostatic potential "orbitals" for two nearby spheres. Antisymmetric and symmetric modes are shown. The antisymmetric mode is dipole active. A molecular dipole is indicated by the arrow. (e) Some higher excitation modes for the electrostatic potentials "orbitals".

those of the individual spheres by superimposing their respective electric field patterns. Here the language of molecular orbital theory may be used, although it must be remembered that electrostatic potentials, rather than electronic wavefunctions, are being analyzed. In place of atomic eigen-energies we now have the sphere resonances, which occur when $\epsilon = -(l+1)/l$, l being the order of the Legendre polynomial associated with a given excitation. In place

of atomic eigenfunctions we now have electrostatic potentials, which fall off as r^{-l-1} away from the spheres. The fundamental excitation of a sphere is the dipolar excitation ($l = 1$). As two spheres are brought into proximity the overlapping "orbitals" will form σ and π "bonds". The strongest degree of electrostatic coupling occurs for the σ bond composed of two dipolar excitations. The resonant frequency of this mode is red-shifted away from the isolated sphere resonances. Unless the spheres are practically touching, the higher-lying "molecular" states should lie in the vicinity of the sphere resonances, since the degree of "hybridization" can be expected to be small. An illustration of several low-lying modes is given in figs. 2d and 2e. A molecule located at position "A" may be expected to couple strongly to the red-shifted σ-mode and not as strongly to the higher modes. Likewise, a molecule at position "B" may be expected to couple weakly to all modes.

In fig. 3 we display results obtained from a Green function calculation [46] for two silver spheres separated by a gap equal a fifth of the radius of a sphere. The intensity enhancement factor is plotted as a function of the frequency. The frequency of the red-shifted σ-orbital is denoted by "σ" and the location of the sphere modes are denoted by $l = 1, 2, \ldots$. When the molecule is at position A we see that the σ-orbital is readily excited and the higher modes less prominently excited. When at position B, all modes are only weakly excited, due to the inefficient coupling of the dipole to the electric field of the sphere modes.

The effect of an underlying substrate on these considerations may be understood as follows. The resonant frequency of a localized mode of the

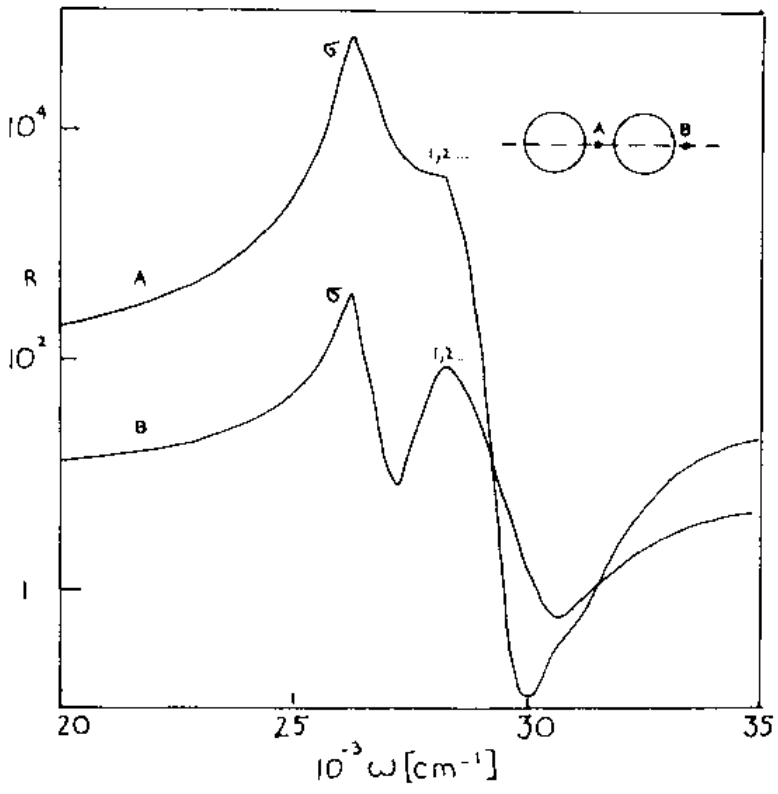

Fig. 3. Intensity enhancement factor versus photon frequency. The red-shifted mode is denoted by σ and the isolated sphere modes by $l = 1, 2, \ldots$. The inset describes the geometry.

cluster will be degenerate with the frequency of some delocalized plasmons of the substrate. Energy from the cluster will therefore be lost in radiation to these surface plasmons and consequently the the cluster resonances will be broadened [50]. Similarly, coupling to photon radiation by the cluster will also lead to additional broadening. The absolute values of the enhancement factors will therefore be somewhat diminished, but the relative values at different portions of the cluster should not be affected. The fact that the cavity sites are locations which are both associated with strong coupling to the red-shifted mode and associated with strong local fields helps explain why the SERS spectrum is often found to be red-shifted from the absorption spectrum. The absorption spectrum comes about from an excitation of dipolar modes of all particles in the system – whether they be clustered or unclustered. Unclustered configurations will respond at the sphere resonances and will be unshifted in frequency. The SERS spectrum is dominated by those modes and sites associated with the strongest local fields such as cavity sites and hence will be red-shifted.

In summary we have the following observations: (a) A collection of spheres has strong local fields in the inter-sphere regions. (b) A collection of spheres possesses a resonance which is shifted towards the red from that of an isolated sphere. (c) When the spheres are in the proximity of a substrate the resonances will be broadened due to surface plasmon emission. Otherwise they are broadened only by radiative damping and the usual local heating effects.

4. Absorption, resonance Raman scattering and luminescence

Resonance optical processes, of which absorption, resonance light scattering and luminescence (i.e. fluorescence and phosphorescence) are the lowest order (in the molecule–radiation field interaction) examples are affected by both the surface-induced local field enhancement and the surface-induced relaxation. This is in contrast to nonresonant processes such as regular Raman scattering which are influenced only by the local field. The reason for this becomes obvious by considering eq. (4). The induced molecular dipole is seen to be proportional to the local field $(I + A)\cdot E_0$ and inversly proportional to

$$\left(\omega_M^0 + \Delta\omega_M^{(s)}\right)^2 - \omega^2 - i\omega\left(\gamma_M^0 + \gamma_M^{(s)}\right).$$

Far from resonance the term containing the surface modified width may be disregarded while at resonance the induced dipole is proportional to

$$(I + A)\cdot E_0 / \left[\omega\left(\gamma_M^0 + \gamma_M^0 + \gamma_M^{(s)}\right)\right].$$

Since in many situations $|A| > 1$ the surface effect on the local field and on the relaxation rate are seen to change the induced molecular dipole in opposite

directions. The level width dominates the surface effect for small surface–molecule distances while the local field enhancement dominates it at larger distances. This gives rise to nontrivial distance dependence of the cross-section under discussion. We now discuss the different processes in more detail.

4.1. Absorption

The absorption cross-section is easily obtained in the oscillating dipole model of section 2. Starting from:

$$\boldsymbol{E}_0(\boldsymbol{R}_M, t) = \eta_0 \cos(\omega t + \phi_0), \tag{8}$$

and using eq. (4a), we obtain

$$\mu(t) = \tfrac{1}{2}\left[\mu(\omega)\, e^{-i(\omega t+\phi_0)} + \mu^*(\omega)\, e^{i(\omega t+\phi_0)}\right], \tag{9}$$

where

$$\mu(\omega) = \frac{\alpha_M \omega_M^2}{\omega_M^2 - \omega^2 - i\omega\gamma_M} \boldsymbol{n}_\mu \cdot \left[I + A(\boldsymbol{R}_M, \omega)\right] \cdot \eta_0. \tag{10}$$

η_0 is the amplitude of the incident field at the position of the molecule and ϕ_0 is its phase. The energy absorbed per unit time by the molecule is

$$\dot{W}_M^{(ab)} = \dot{\mu}(t)\left\{\boldsymbol{n}_\mu \cdot \left[I + A(\boldsymbol{R}_M, \omega)\right] \cdot \boldsymbol{E}_0(\boldsymbol{R}_M, t)\right\}. \tag{11}$$

Inserting eqs. (8)–(10) into (11) yields

$$\dot{W}_M^{(ab)} = \left|\boldsymbol{n}_\mu \cdot \left[I + A(\boldsymbol{R}_M, \omega)\right] \cdot \eta_0\right|^2 \frac{\omega^2 \omega_M^2 \alpha_M \gamma_M}{\left(\omega_M^2 - \omega^2\right)^2 + \omega^2 \gamma_M^2}. \tag{12}$$

If we set $\omega = \omega_M + \Delta\omega$ and expand in $\Delta\omega$, and if we further divide by the incident flux $C|\eta_0|^2/8\pi$ we obtain the absorption cross-section in the form

$$\sigma_{ab} = \tfrac{3}{2}(2\pi c/\omega_M)^2 \Gamma_R^{(f)} \left|\boldsymbol{n}_\mu \cdot \left[I + A(\boldsymbol{R}_M, \omega)\right] \cdot \boldsymbol{n}_E\right|^2 \frac{\gamma_M/2\pi}{(\Delta\omega)^2 + (\gamma_M/2)^2}, \tag{13}$$

where $\boldsymbol{n}_E = \boldsymbol{n}_0/n_0$ is a unit vector in the direction of the incident field and where we have used eq. (1) to relate α_M to the free radiative lifetime $\Gamma_R^{(f)}$.

The resulting expression (13) for the absorption cross-section is similar in form to that of a free molecule (of a given orientation relative to the field) with two important differences: First, the surface-induced local field correction changes σ_{ab} by a factor

$$\left|\boldsymbol{n}_\mu \cdot \left[I + A(\boldsymbol{R}_M, \omega)\right] \cdot \boldsymbol{n}_E\right|^2 / (\boldsymbol{n}_\mu \cdot \boldsymbol{n}_E)^2.$$

This change may become a substantial enhancement for ω near a surface plasmon resonance or near a sharp tip parallel to the incident field (lightning

rod effect). Secondly the width γ_M (and the resonance frequency ω_M) in (13) contains the surface contribution. This leads to a reduction of σ_{ab} on resonance ($\Delta\omega = 0$) by a factor $\gamma_M^0/(\gamma_M^0 + \gamma_M^s)$. (Recently Metiu and Das [31] have presented results of a calculation which lead to an additional factor γ_M^0/γ_M^s in σ_{ab}. Since often $\gamma_M^0 \ll \gamma_M^{(s)}$ this seems to indicate that σ_{ab} is reduced even further. Discusions with these authors have lead to the conclusion that the result (13) is indeed the correct one.)

Finally it is important to note that the surface-induced corrections to γ_M and ω_M depend on the incident frequency ω, so that the lineshape (13) is not necessarily a Lorentzian. An example is shown in fig. 2.

4.2. Resonance Raman scattering and fluorescence

The simplest description of resonance Raman scattering, resonance fluorescence and regular luminescence (fluorescence or phosphorescence) is given by the four-level model of fig. 4 [5]. $|g\rangle$ is the ground molecular state, $|g'\rangle$ is an excited vibrational level of the ground electronic manifold. $|0\rangle$ and $|1\rangle$ are the ground and excited vibrational levels of an excited electronic manifold. The incident light of frequency ω is near resonance with the $|g\rangle \rightarrow |1\rangle$ transition. The near resonance condition makes it possible to disregard excited levels other than $|1\rangle$ and levels which are populated thermally following the excitation of $|1\rangle$. The resonance Raman component of the outgoing radiation is the light scattered prior to any thermal interaction by the molecule in the intermediate level $|1\rangle$. Resonance fluorescence is the emission from the molecule in level $|1\rangle$ following thermal phase relaxation (dephasing) in which the molecule forgets its excitation history. Regular fluorescence is the emission from level $|0\rangle$ following thermal population relaxation. (Level $|0\rangle$ may belong to a different excited electronic state. When this is a triplet the $|0\rangle \rightarrow |g'\rangle$ emission is phosphorescence. We continue to use the word fluorescence in the following discussion.)

The theory of resonance light scattering and luminescence from thermally relaxing systems [5,47] yields, within the impact approximation, the following expression for the emitted radiation

$$\sigma \sim \frac{|V_{g1}V_{1g'}|^2}{(\omega-\omega_{1g})^2+(\gamma_1/2)^2}\left[\delta(\omega_{g'g}-\omega+\omega')+\frac{\kappa_1}{\gamma_1-\kappa_1}\frac{\gamma_1/2\pi}{(\omega'-\omega_{1g'})^2+(\gamma_1/2)^2}\right.$$
$$\left.+\left|\frac{V_{g'0}}{V_{g'1}}\right|^2\frac{T_{01}}{T_{10}+\Gamma_0}\frac{\gamma_1}{\gamma_1-\kappa_1}\frac{\gamma_0/2\pi}{(\omega'-\omega_{0g'})^2+(\gamma_0/2)^2}\right] \qquad (14)$$

where $V_{ab} = \mu_{ab}\chi_{ab}$ ($a, b = 0, 1$) is a product of the transition dipole μ_{ab} and a Franck–Condon factor χ_{ab} associated with the $|a\rangle \rightarrow |b\rangle$ transition, $\omega_{ab} =$

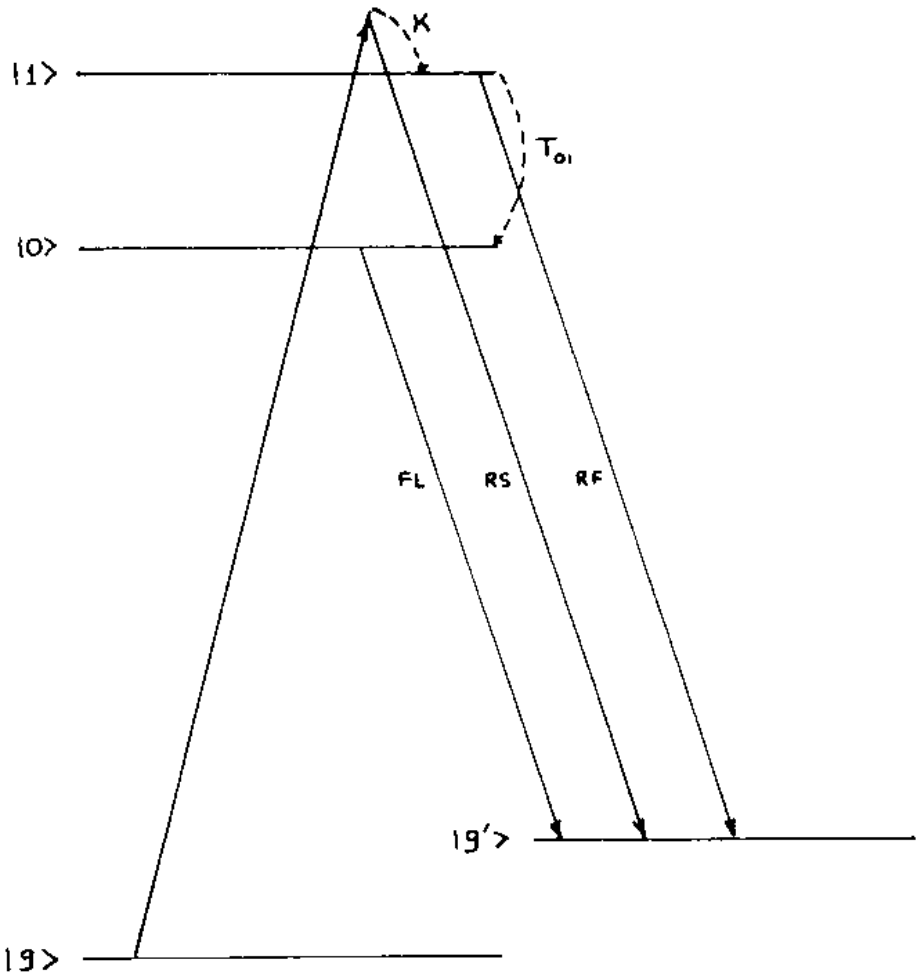

Fig. 4. Energy levels and transitions for the four-level model of resonance Raman scattering and fluorescence. Dashed lines represent nonradiative processes. Solid lines represent radiative transitions: absorption, Raman scattering (RS), resonance fluorescence (RF) and regular (relaxed) fluorescence (FL).

$(E_a - E_b)/\hbar$, γ is the total level width, e.g.,

$$\gamma_1 = \kappa_1 + \Gamma_1 + T_{01}\left[1 - T_{10}/(T_{10} + \Gamma_0)\right], \tag{15}$$

where κ_1 is the dephasing rate and Γ_1 (including radiative Γ_1^{R} and nonradiative Γ_1^{NR} contributions) is the population relaxation rate of level $|1\rangle$, not including its interaction with level $|0\rangle$. T_{ab} is the rate of thermal population transfer from level b to level a. The result (14) is obtained by disgarding possible interference effects between level $|0\rangle$ and $|1\rangle$.

The three terms in eq. (14) correspond to the resonance Raman, resonance fluorescence and the regular fluorescence contributions. The corresponding results near a dielectric surface is obtained [5] by multiplying σ by the local field enhancement factor corresponding to the incoming (ω) and outgoing (ω') frequencies (the tensor notation is suppressed for simplicity) and by replacing Γ_a ($a = 1, 2$) by $\Gamma_a + \Gamma_a^{(\mathrm{s})}$ where $\Gamma_a^{(\mathrm{s})}$ is the surface contribution to the relaxation rate. This leads [5] to the following enhancement ratios for the different processes

$$R_{\mathrm{RS}} = |[1 + A(\omega)][1 + A(\omega')]|^2, \tag{16}$$

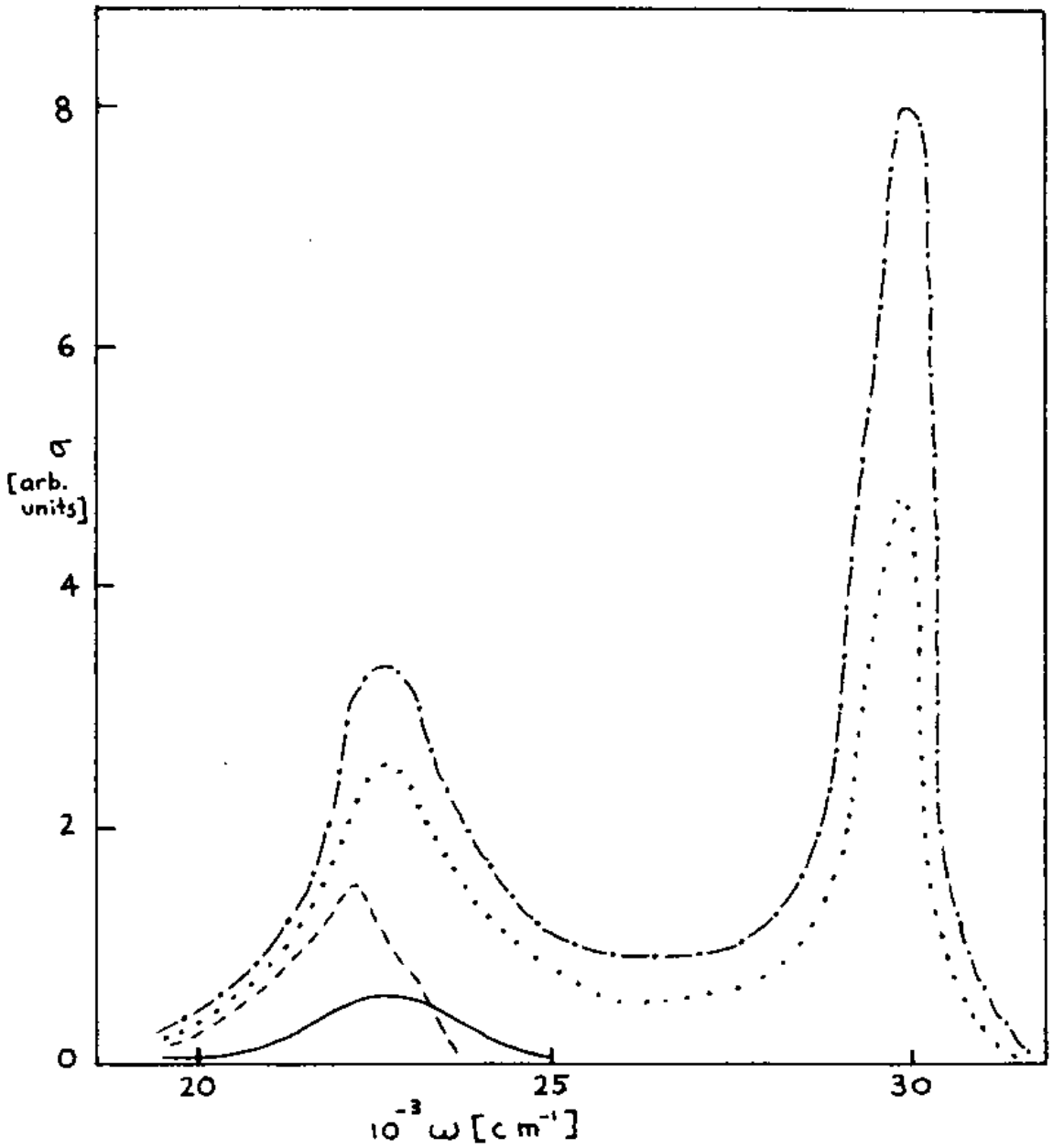

Fig. 5. Absorption cross-section for a model I_2 molecule near silver and gold spheres of radius 500 Å. The molecule is perpendicular to the sphere surface and is oriented parallel to the incident electric field. (———), free molecule; (— — —), molecule at a distance 5 Å from a gold sphere; (· · · · · ·), molecule at a distance 50 Å from a silver sphere; (– · –), molecules at a distance 5 Å from a silver sphere.

$$R_{\mathrm{RRS+RF}} = R_{\mathrm{RS}} \frac{\gamma_1}{\gamma_1 + \Gamma_1^{(s)}} \frac{\Gamma_1 + \mathrm{T}_{01}}{\Gamma_1 + \mathrm{T}_{01} + \Gamma_1^{(s)}}, \tag{17}$$

$$R_{\mathrm{FL}} = R_{\mathrm{RRS+RF}}\, \Gamma_0 / \left(\Gamma_0 + \Gamma_0^{(s)}\right). \tag{18}$$

R_{RS} is the enhancement ratio associated with the regular (nonresonant) Raman scattering. For simplicity we have assumed that the thermal relaxation rates R and T are not modified by the surface. Also, we have considered the resonance Raman and resonance fluorescence contributions together because in most experimental situations they cannot be resolved. The results (16)–(18) lead to the following conclusions:

(1) Resonance processes may be enhanced near the surface but to a lesser degree then nonresonant processes. The latter are modified mostly by the local field while the former are reduced by the surface-induced decay. Regular fluorescence is enhanced (if at all) less than the resonance emission. It should be noted that the enhancement ratio (17) for the resonance scattering is the ratio between the cross-sections of this process on the surface and in the bulk. The resonance signal is of course much stronger than the regular Raman signal because of the resonance enhancement.
(b) The observation of enhancement (or reduction) depends on the yield of the observed resonance process in the free molecule. Processes involving molecules of small quantum yields (large Γ^{NR}) are expected to be enhanced more strongly then those of high quantum yield (small Γ^{NR}) because when Γ^{NR} is large the effect of $\Gamma^{(s)}$ is smaller in eqs. (17), (18) and the local field enhancement dominates.
(c) The resonance enhancement ratios are expected to go through a maximum as functions of the molecule–surface distance. For small separations $\Gamma^{(s)}$ is very large and may cause a reduction in the emission cross-section relative to that of the free molecule. As the molecule–surface separation increases, the dominant, nonradiative, contribution in $\Gamma^{(s)}$ vanishes much more quickly than the local field enhancement. At intermediate separations (~ 0.1–0.2 of the roughness scale) the latter dominates and the enhancement ratio is maximal.

These qualitative predictions are all confirmed by experimental observations. A lower surface enhancement of resonance Raman scattering and fluorescence has been observed by several workers [4–6]. The distance dependence of the luminescence yield has been studied by Wokaun et al. [10] and found to be in close agreement with the theoretical prediction.

4.3. *The apparent yield*

Having access to the radiative and nonradiative lifetimes Γ^{R} and Γ^{NR} of the excited molecular state, the emission yield is defined from

$$Y_{FL} = \Gamma^{R}/(\Gamma^{R} + \Gamma^{NR}). \tag{19}$$

However, the emission intensity is often monitored for a fixed incident intensity while some structure parameter is varied. This emission intensity is not normalized by the absorbed energy and we call it the apparent yield [20]. The enhancement ratios (17) and (18) are ratios between such quantities calculated for molecules on the surface and in the bulk. Similar ratios between the real yields are obtained by diviidng eqs. (17) and (18) by $|1 + A(\omega)|^2$ to eliminate the effect of the increased local field.

4.4. *Coverage effects*

As discussed in section 1, high adsorbate coverages which affect also the regular SERS [36] lead to a substantial change in the optical response of the

substrate–adsorbate system near resonance of the adsorbate. We refer to the literature [7,9,36–39] for discussions of these effects.

4.5. Choice of substrate

SERS is notably strong in the coinage metals (Ag, Cu, Au) and has been reported on some other substrates. For processes involving resonance transitions in the adsorbate molecule, strong electromagnetic effects of the substrate are expected only when the molecular resonance is not too far from the surface plasmon resonances. This makes the choice of substrate much more crucial in the resonance case. See ref. [11] for a discussion of this issue.

4.6. Nonlinear processes

Our discussion above focused on processes which are linear in the incident field. The enhanced local field near the surface may give rise to nonlinear optical processes, as observed by Glass et al. (two-photon fluorescence from rhodamine 6G on a silver particle film [7b]) and by Shen and co-workers (second harmonic generation by adsorbed molecules) [48]. The electromagnetic theory of these processes is similar in spirit to that for linear optical processes, with the local field enhancement factor entering in the proper power. It should be mentioned that another source of nonlinearity is the very large gradient of the local field near the surface [49].

5. Resonance optical response of small clusters

When considering the physical effects associated with small particles (10–10000 Å in size) one is looking at a domain which is neither microscopic nor macroscopic. It is not microscopic in the sense that quantum-chemical calculations get to be beyond the capacity of even the largest computers available. It is not macroscopic because while the number of atoms involved is large it is still finite. In principle finite-size effects associated with quantum mechanics can play a role. Furthermore the surface to volume ratio is fairly large, so a larger relative role is played by the surface. In addition, fluctuation effects are likely to be more pronounced, since the number of particles is finite.

Quantum size effects have been the focus of considerable attention, primarily as they relate to metallic particles, and will not be considered here. The role of surface screening has been considered recently as it relates to the infrared region of the spectrum [54]. In this section we will focus our attention primarily on dielectric particles and study fluctuation effects. The fluctuations to be considered are either spatial fluctuations or temporal fluctuations.

In studying macroscopic systems it is conventional to describe the electrical properties in terms of certain macroscopically averaged quantities, such as the

dielectric constant. This quantity may be either regarded as a nonlocal function or, when considering a class of phenomena, as a local function. In either case, however, it is assumed that there are a sufficient number of particles present so that the spatial and temporal fluctuations are of little consequence. However, when dealing with a cluster with a finite number of particles, atomic motions could cause the density in one part of the particle to be somewhat different from that in another part of the particle. In the same way the random motion of the atoms could cause transients in the local density. Some parameters of the system are particularly sensitive to these spatial or temporal fluctuations. For example, the energy spacing between two atomic levels can be strongly influenced (shifted and/or broadened) by neighboring atoms. If we are studying the system far from resonance the effect of the fluctuations is not too serious. But in the vicinity of resonance the effects are important.

The basic equation of our theory is based on a rotating wave approximation for the individual molecular dipoles

$$\dot{\mu}_j + \left[i\omega_0 + i\phi_j(t) + \tfrac{1}{2}\gamma\right]\mu_j = \tfrac{1}{2}i\omega_0\alpha_0\left(E_{ex}\,e^{-i\omega t} + \sum_{j'} M'_{jj'}\cdot\mu_{j'}\right). \tag{20}$$

Included in this expression is a frictional damping, γ, the effect of dephasing, described by a random fluctuation phase $\phi_j(t)$, interparticle coupling, described by a spatially dependent tensor $M_{jj'}$ and an external driving field, E_{ex} at ω. Here ω is the natural frequency of the oscillator and α_0 is the DC polarizability. The phases $\{\phi_j(t)\}$ are taken to be delta-correlated Gaussian random variables with zero mean and fluctuation strength κ. Our results may be summarized as follows [55]:

(a) When we are interested in the properties of the mean dipole (and hence the mean dielectric function) the above equation may be simplified to

$$\langle\dot{\mu}\rangle + \left[\left(i\omega + \tfrac{1}{2}\Gamma\right)I - \tfrac{1}{2}i\omega_0\alpha_0 M\right]\langle\mu\rangle = \tfrac{1}{2}i\omega_0\alpha_0 E_{ex}\,e^{-i\omega t}, \tag{21}$$

where now μ denotes a $3N$-dimensional vector. Here $\Gamma = \gamma + \kappa$, so the dephasing process simply induces an additional damping rate, a result previously known for a single oscillator but now generalized to a system of interacting molecules.

The effect of clustering may be taken into account by performing a virial expansion. This allows us to develop a power series in the molecular density and to obtain higher-order density corrections to the usual Clausius–Mossotti formula.

(b) When we are interested in discussing a higher-order process, e.g., light scattering or nonlinear effects, it is not $\langle\mu\rangle$ which is of primary importance but rather the autocorrelation function $\langle\mu(t)\cdot\mu(t')\rangle$. It is still possible to evaluate this function in the framework of either Gaussian random variable theory or density matrix theory. This leads to an expression for the light scattering which

includes both coherent and incoherent contributions. The coherent contributions are describable in terms of the mean dipole, and hence in terms of a dielectric function. The incoherent contributions are due to the temporal fluctuations and are not describable purely in dielectric terms. The ratio of the coherent to the incoherent terms in the cross-section for scattering goes as [55]

$$\sigma_{\text{coherent}}/\sigma_{\text{incoherent}} = N\gamma/\kappa, \tag{22}$$

and hence grows as the number of particles grows. Thus, typically, for $N \gtrsim 10^4$ the coherent behavior dominates and a dielectric description is adequate. For $N \lesssim 10^4$, however, incoherent terms are also important.

6. Photochemistry

In section 4 we discussed resonance emission from molecules adsorbed on rough dielectric surfaces and on dielectric particles. The same factors which determine the surface effect on these processes also govern the yield of nonradiative processes which follow the molecular excitation. Of these, photochemistry is potentially the most useful. Nitzan and Brus [11] have studied theoretically different aspects of surface-enhanced photochemistry coming to conclusions similar to those related to resonance Raman scattering and to fluorescence:

(a) Photochemical processes may be enhanced on rough dielectric surfaces or on dielectric particles, provided the surface resonance response is close in frequency to the molecular absorption peak. (This statement should be modified in case of two- or more-photon excitation.) This enhancement results from the enhanced local electromagnetic field near the surface.

(b) The apparent photochemical yield depends on the competing surface effects: local field enhancement and surface-induced relaxation.

(c) The enhancement of photochemical processes will be more pronounced when the rate of the chemical process involving the excited molecule is very large so as to compete effectively with the surface-induced damping. This is the case, e.g., for direct photodissociation. The photodissociation of the iodine molecule is a possible candidate for study. Theoretical estimates [11] predict large enhancements of this process on all the coinage metals, particularly on rough silver surfaces with a roughness scale of a few hundred Å. (Note that I_2 reacts with these metals so some inert spacer is necessary.) Another case where the surface enhancement is expected to be more pronounced is when another nonradiative process competes effectively with both the photochemical channel and with the surface-induced damping. In this case the photochemical yield will be very low in the bulk, but will increase with the local field intensity without being adversely affected by the surface-induced damping.

(d) Infrared photochemistry is predicted [11] to be enhanced on appropriately chosen ionic or small-band semiconductor surfaces.

(e) Photochemistry will generally be less enhanced then other resonance processes which involve both incident and emitted radiation. The enhancement ratios (16)–(18) are all proportional to

$$|(1+A(\omega))(1+A(\omega'))|^2,$$

where $A(\omega)$ is the factor introduced in eq. (3) and where ω and ω' are the incident and emitted frequencies. Photochemical and other nonradiative processes are enhanced only by the $|1+A(\omega)|^2$ factor associated with the enhancement of the incident field.

(f) The dependence of the apparent photochemical yield on the molecule–surface separation is similar to that discussed in section 4 for RRS and RF. Unless the photochemical reaction (or some other radiationless process involving the excited molecule) competes effectively with the surface-induced damping (which is almost never true for molecules adsorbed directly on a metal surface) the photochemical yield is predicted to be maximum at some finite separation (10–50 Å for a 200 Å silver sphere). In fact, the surface-induced damping is so fast for the first monolayer on metal surfaces ($\sim 10^{15}$ s^{-1} for allowed molecular transitious) that most photochemical processes will not proceed during this short lifetime.

Recent experimental reports confirm these predictions. Goncher and Harris [12] have observed enhanced photodecomposition of pyridine, pyrazine and benzaldehyde on Ag(110) roughnened by Ar sputtering. (Negative results were obtained with benzene, cyclohexane and acetophenone.) This effect was shown to be long ranged using NH_3 as spacer. Garoff, Weitz and Alverez [56] have observed the opposite effect: A monolayer of rhodamine 6G deposited on Ag island film on silica was shown to be more stable to photodegradation on the Ag than on the silica. Evidently the rapid energy transfer from the excited molecule to the Ag blocks the photochemical channel in this case.

Another class of experiments is exemplified by the work of Chen and Osgood [13] who used a frequency-doubled Ar ion laser beam (257 nm) to irradiate Me_2Cd vapor in the presence of small (10–300 nm) Cd and Au spheres. The Cd particles grow into ellipsoids with their long axis in the direction of the incident field. The growth stops after the ellipsoids reach an aspect ratio ~ 1.8 (long axis ~ 110 nm) persumably because beyond this size and shape their optical resonance was far from the transition that affects the Me_2Cd decomposition. Au particles do not show an effect at this wavelength, presumably for the same reason.

A series of experiments of a similar nature is the laser deposition of metals from organometallic vapors on solid surfaces [57,58] (mostly silica). Under certain conditions periodic structure in the deposited film is observed. This may be explained [56] by the generation of surface plasmon waves which leads to enhancement of the photochemical rate in a pattern which follows the periodicity of the local field. This periodicity results from the interference between the incident laser beam and the surface plasma wave.

The experimental results described above indicate that surface-enhanced photochemistry is potentially a useful tool for controlling chemical processes on dielectric surfaces. It is of interest to study possible applications for surface microfabrication, selective photochemical catalysis and multiphoton chemistry.

7. Energy transfer

The transfer of energy from a donor to an acceptor molecule is fundamental to the understanding of the relaxation of an excited state and the deposition and distribution of energy in solids, liquids and gases. A well-studied mechanism for this energy transfer in the Forster–Dexter mechanism [59]. In this process an initially excited donor molecule (D) becomes de-energized while an initially relaxed acceptor molecule (A) becomes energized. The interaction proceeds, to lowest order, through a dipole–dipole coupling and concise expressions based on Fermi's golden rule may be obtained. The interactions, being of a long-ranged character, produce energy transfer over sizeable distances, with 50 Å being typical. The energy transfer is usually regarded as taking place in a passive and inert environment. In our work [15] we have sought to study what happens if the environment takes on a more active role. Can the environment assist in the energy-transfer process and, for example, speed up the transfer rates or extend the range over which energy transfer may occur? The answer to these questions may be of fundamental importance, for example in the utilization of energy from electromagnetic waves or in photovoltaic applications.

As a simple model for enhanced energy transfer let us suppose that the donor and acceptor molecules lie in the vicinity of a solid state particle (or collection of particles) whose resonance bands overlap those of the donor and acceptor. It is then possible for energy to be first transferred to the particle (or particles) and then finally to the acceptor. We know from our work on local fields near spheriodally shaped particles that a small dipole on a donor molecule may induce a giant dipole on the particle. The field of this giant dipole may couple to neighboring acceptor dipoles and complete the energy transfer.

A simple way to discuss the effect is to regard the particle as enhancing the dipole–dipole interaction between the donor and acceptor pair. An analytic formula for the case of two molecules near a spheroidal particle may be obtained. Since the Fermi golden rule predicts that the energy-transfer rate is proportinal to the square of this enhancement factor, one may directly predict the size of the effect. What is found are: (a) the range of the energy transfer may be extended to several hundred ångströms, or even more, depending on the size of the particle and its shape; (b) the timescale for the energy to be transferred is cut down by several orders of magnitude due to the enhanced

dipole–diople coupling; (c) the presence of the particle opens up competing channels for energy deposition and thus may strongly affect the yield for energy transfer.

Based on our previous discussion involving local fields and cavity sites one may argue that efficient locales for donors and/or acceptors would be the cavity sites for a surface or the inter-sphere sites (for a colloid). It is precisely at these locations where a strong global dipole, and hence the possibility for efficient communication between molecules, may occur.

In the case of two molecules located along the axis of a prolate spheroidal particle but on opposite sides of it, the expression for the energy-transfer rate may be written as

$$k = |A(\omega)|^2 k_0, \tag{23}$$

where k_0 is the Forster–Dexter expression, which is proportional to r^{-6} (r

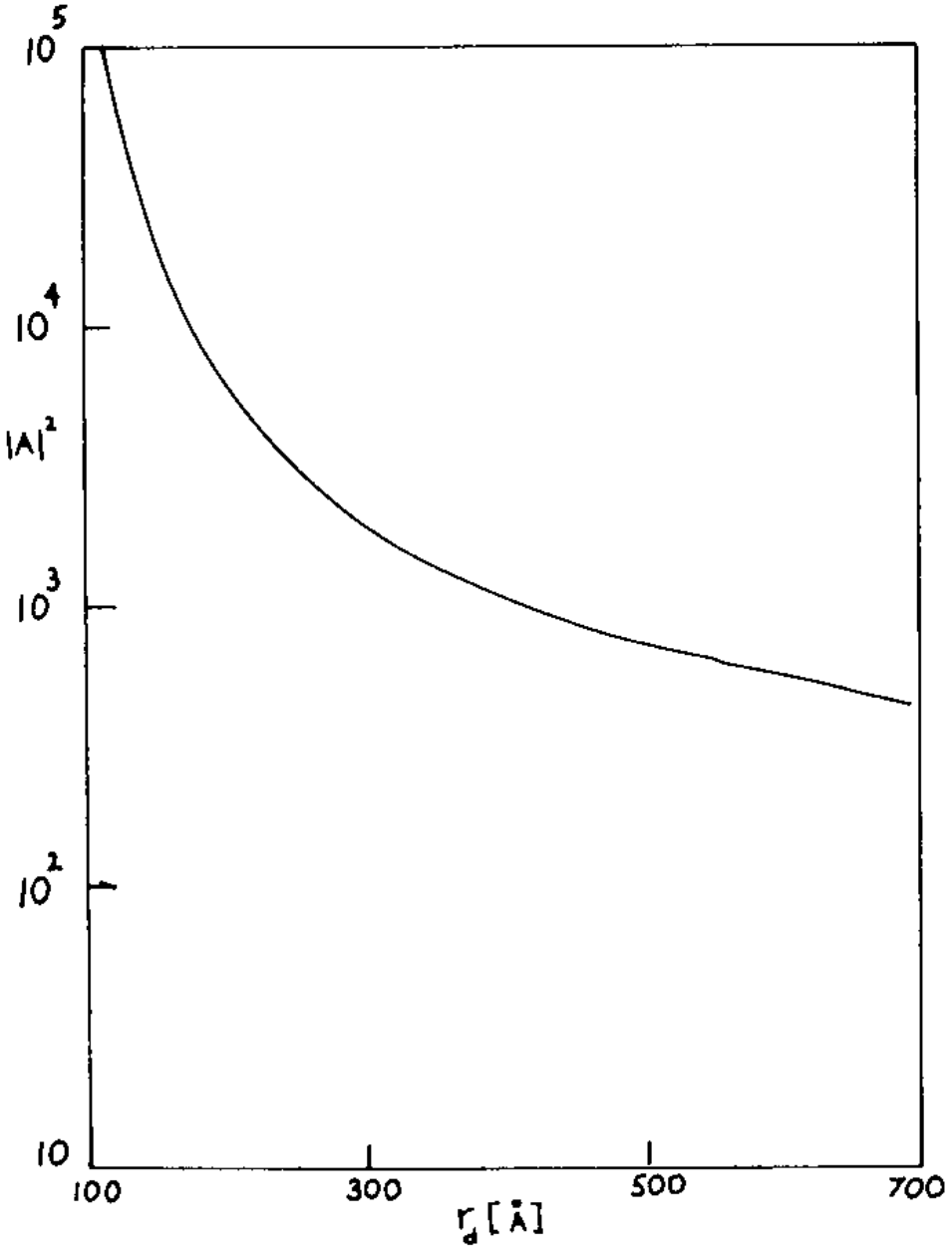

Fig. 6. Energy-transfer rate enhancement ratio versus donor location for fixed acceptor location.

being the donor–acceptor separation), and $A(\omega)$ is an amplification factor now given by [15]:

$$A(\omega) = 1 + \sum_{n=1}^{\infty} (-)^n \left(n + \tfrac{1}{2}\right) \frac{1-\epsilon}{\epsilon + \bar{\epsilon}_n} \frac{P_n(\xi_0)}{Q_n(\xi_0)} Q_n'(\xi_d)\, Q_n'(\xi_a)\, (\xi_d + \xi_a)^3. \quad (24)$$

Here P_n and Q_n are Legendre functions, ϵ is the frequency-dependent dielectric constant of the medium and $\xi_0 = a/f$, $\xi_d = r_d/f$, $\xi_a = r_a/f$, where $f = (a^2 - b^2)^{1/2}$. The semi-major axis of the spheroid is a, the semi-minor axis is b,

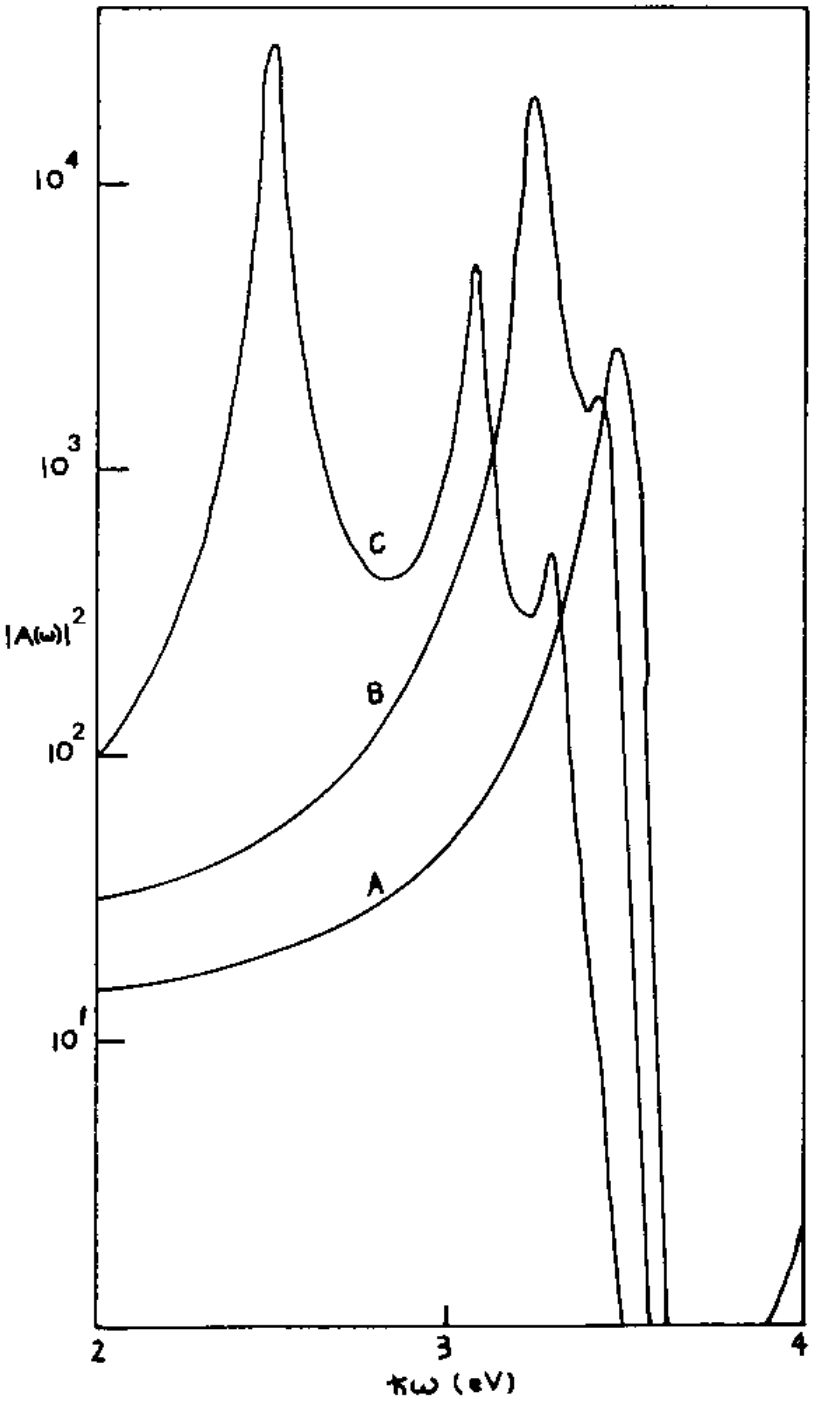

Fig. 7. Energy-transfer rate enhancement ratio versus photon energy for several shapes of the spheroid.

and the distances of the molecules from the center are r_d and r_a. The quantity $\bar{\epsilon}_n$ is defined by

$$\bar{\epsilon}_n = -P_n(\xi_0)\, Q_n'(\xi_0)/Q_n(\xi_0)\, P_n'(\xi_0). \tag{25}$$

A plot of $|A(\omega)|^2$ versus donor location for fixed acceptor location is presented in fig. 6. The graph is for a silver spheroid with $a = 100$ Å and $b = 64$ Å with the transition energy resonating with the spheroid at 3.25 eV. The donor was held fixed at $r_d = 150$ Å. We see from this figure that the enhancement of the energy-transfer rate is a long-ranged phenomenon and that it is also quite strong, particularly as the donor gets close to the particle.

In fig. 7 we present a graph of the intensity enhancement factor $|A(\omega)|^2$ versus photon energy for several prolate silver spheroids. Here $a = 100$ Å and $r_a = r_d = 150$ Å. In curve A, $b = 95$ Å; in B, $b = 64$ Å; and in C, $b = 30$ Å. Note the shift of the location of the resonance with varying aspect ratio a/b. As the spheroid gets sharper, the most prominent peak shifts to the red. Also note the presence of additional resonances due to the higher excited states of the particle. Finally note the slow growth of maximum intensity with increasing sharpness, despite the fact that the particle volume is increasing.

8. Summary

In summary, we see that the photophysics and photochemistry of molecules near surfaces or small particles is significantly affected by electrodynamic interactions. Quantitative calculations for these interactions can be made by treating the surfaces or small particles as dielectric materials subject to the macroscopic Maxwell equations. The major factors influencing such properties as SERS, fluorescence rates and yields, absorption cross-sections, photochemistry, and energy-transfer rates are the strong local fields and the resonances of the dielectric medium. We have also studied possible limitations on the dielectric theory and find that it is valid for all but the very small particles. Thus we conclude that macroscopic electrodynamics is an important factor influencing photochemistry and photophysics near surfaces.

References

[1] For reviews on various aspects of SERS, see R.K. Chang and T.E. Furtak, Eds., Surface Enhanced Raman Scattering (Plenum, New York, 1981).

[2] For a review, see R.R. Chance, A. Prock and R. Silbey, in: Advances in Chemical Physics, Vol. 37, Eds. I. Prigogine and S.A. Rice (Wiley, New York, 1978) p. 1. More recent developments which take into account the nonlocal nature of the dielectric response of the substrate are given in ref. [3].

[3] Ph. Avouris and B.N.J. Persson, J. Phys. Chem. 88 (1984) 837.
[4] A.M. Stacy and R.P. Van Duyne, Chem. Phys. Letters 102 (1983) 365.
[5] D.A. Weitz, S. Garoff, J.I. Gersten and A. Nitzan, J. Chem. Phys. 78 (1983) 5324.
[6] A. Bachackashvilli, S. Efrima, B. Katz and Z. Priel, Chem. Phys. Letters 94 (1983) 571.
[7] (a) A.M. Glass, P.F. Liao, J.G. Bergman and D.H. Olson, Opt. Letters 5 (1980) 368;
(b) A.M. Glass, A. Wokaun, J.P. Heritage, J.G. Bergman, P.F. Liao and D.H. Olson, Phys. Rev. B24 (1981) 4906.
[8] G. Ritchie and E. Burstein, Phys. Rev. B24 (1981) 4843.
[9] D.A. Weitz, S. Garoff, C.D. Hanson, T.J. Gramila and J.I. Gersten, J. Luminescence 24/25 (1981) 83.
[10] A. Wokaun, H.P. Lutz, A.P. King, U.P. Wild and R.R. Ernst, J. Chem. Phys. 79 (1983) 509.
[11] A. Nitzan and L.E. Brus, J. Chem. Phys. 74 (1981) 5321; 75 (1981) 2205.
[12] G.M. Gonscher and C.B. Harris, J. Chem. Phys. 77 (1982) 3767.
[13] C.J. Chen and R.M. Osgood, Phys. Rev. Letters 50 (1983) 1705.
[14] M. Moskovits, private communication.
[15] J.I. Gersten and A. Nitzan, Chem. Phys. Letters 104 (1984) 31.
[16] S. Efrima and H. Metiu, J. Chem. Phys. 70 (1979) 1602, 1939, 2297; Surface Sci. 92 (1980) 417.
[17] F.W. King, R.P. Van Duyne and G.C. Schatz, J. Chem. Phys. 69 (1978) 4472.
[18] M. Moskovits, J. Chem. Phys. 6 (1978) 4159; Solid State Commun. 32 (1979) 59.
[19] J.I. Gersten, J. Chem. Phys. 72 (1980) 5779;
J.I. Gersten and A. Nitzan, J. Chem. Phys. 73 (1980) 3023.
[20] J.I. Gersten and A. Nitzan, J. Chem. Phys. 75 (1981) 1139.
[21] S.L. McCall, P.M. Platzman and P.A. Wolff, Phys. Letters A77 (1980) 381.
[22] D.S. Wang, M. Kerker and H. Chew, Appl. Opt. 19 (1980) 2135, 2256, 4159;
D.S. Wang and M. Kerker, Phys. Rev. B24 (1981) 1777.
The work of this group has been recently reviewed: M. Kerker, Acc. Chem. Res., to be published.
[23] F.J. Adrian, Chem. Phys. Letters 78 (1981) 45.
[24] S.S. Jha, J.R. Kirtley and J.C. Tsang, Phys. Rev. B22 (1980) 3973.
[25] P.K. Aravind, E. Hood and H. Metiu, Surface Sci. 109 (1981) 95.
[26] N.E. Glass, A.A. Maradudin and V. Celli, Phys. Rev. B26 (1982) 5357; B27 (1983) 5150, and references therein.
[27] M. Weber and D.L. Mills, Phys. Rev. B27 (1983) 2698, and references therein.
[28] A. Wirgin and T. Lopez-Rios, Opt. Commun. 48 (1984) 416;
A. Wirgin and T. Lopez-Rios, to be published.
[29] P.K. Aravind and H. Metiu, Chem. Phys. Letters 74 (1980) 301.
[30] J. Arias, P.K. Aravind and H. Metiu, Chem. Phys. Letters 85 (1982) 404.
[31] H. Metiu and P. Das, Ann. Rev. Phys. Chem. 35 (1984) 507.
[32] M. Udagawa, C.C. Chen, J. Hemminger and S. Ushioda, Phys. Rev. B23 (1981) 6843.
[33] A. Campion, J.K. Brown and V.M. Grizzle, Surface Sci. 115 (1982) L153;
A. Campion and D. Mullins, Chem. Phys. Letters 94 (1983) 576;
D.R. Mullins and A. Campion, J. Phys. Chem. 88 (1984) 8.
[34] N. Liver, A. Nitzan and K.F. Freed, J. Chem. Phys., in press.
[35] By "resonance optical processes" we mean processes involving an incident beam near resonance with a transition of the adsorbed molecule.
[36] C.A. Murray and S. Bodoff, Phys. Rev. Letters 52 (1984) 2273.
[37] H.G. Craighead and A.M. Glass, Opt. Letters 6 (1981) 248.
[38] S. Garoff, D.A. Weitz, T.J. Gramila and C.D. Hanson, Opt. Letters 6 (1981) 245.
[39] Z. Kotler and A. Nitzan, J. Phys. Chem. 86 (1982) 2011.
[40] J.E. Demuth and P.N. Sanda, Phys. Rev. Letters 47 (1981) 57.

[41] Ph. Avouris and J.E. Demuth, J. Chem. Phys. 75 (1981) 4783.
[42] J.E. Demuth and Ph. Avouris, Phys. Rev. Letters 47 (1981) 61.
[43] D. Schmeisser, J.E. Demuth and Ph. Avouris, Chem. Phys. Letters 87 (1982) 324.
[44] For a review of the "chemical mechanism" of SERS, see A. Otto, in: Light Scattering in Solids, Vol. 4, Eds. M. Cardona and G. Güntherodt (Springer, New York, 1983).
[45] Some derivations in the literature of the surface-induced level shift and width using a similar procedure use eq. (2) in the form $\ddot{\omega} + (\omega_M^0)^2\omega + \gamma_M^0\dot{\omega} = \omega_M^2\boldsymbol{\alpha}_M \cdot (\boldsymbol{E}_0 + \boldsymbol{R}\cdot\boldsymbol{E}_0 + \mathbf{G}\cdot\mu)$ and derive $\Delta\omega^{(s)}$ and $\gamma^{(s)}$ as tensorial quantities. This is misleading. Obviously for a given transition of a molecule of a given orientation with respect to the surface $\Delta\omega^{(s)}$ and $\gamma^{(s)}$ are scalar quantities.
[46] N. Liver, A. Nitzan and J.I. Gersten, Chem. Phys. Letters 111 (1984) 449.
[47] S. Mukamel and A. Nitzan, J. Chem. Phys. 66 (1977) 2462, and references therein.
[48] P. Ye and Y.R. Shen, Phys. Rev. B28 (1983) 4288, and references therein.
[49] P.R. Antoniewicz, Phys. Rev. B26 (1982) 2285.
[50] P.C. Das and J.I. Gersten, Phys. Rev. B25 (1982) 6281.
[51] E.V. Albano, S. Daiser, G. Ertl, R. Miranda, K. Wandelt and N. Garcia, Phys. Rev. Letters 51 (1983) 2314;
H. Seki and T.J. Chuang, Chem. Phys. Letters 100 (1983) 393.
[52] D.J. Bergman, in: Lecture Notes in Physics, Vol. 154, Eds. R. Burridge, S. Childress and G. Papanicolaou (Springer, Berlin, 1982) p. 10.
[53] P.K. Aravind, A. Nitzan and H. Metiu, Surface Sci. 110 (1981) 189.
[54] X.M. Hua and J.I. Gersten, to be published.
[55] J.I. Gersten and A. Nitzan, Phys. Rev. B29 (1984) 3852.
[56] S. Garoff, D.A. Weitz and M.S. Alvarez, Chem. Phys. Letters 93 (1982) 283.
[57] D.J. Ehrlich, R.M. Osgood, Jr. and T.F. Deutch, IEEE J. Quantum Electron. QE-16 (1980) 1233.
[58] S.R.J. Bruech and D.J. Ehrlich, Phys. Rev. Letters 48 (1982) 1678.
[59] Th. Forster, Ann. Physik 2 (1984) 55; Disc. Faraday Soc. 27 (1959) 7;
D.L. Dexter, J. Chem. Phys. 21 (1953) 836.